Letters

Comprehensive Parameter Optimization Using an Empowered and Lightweight Surrogate Model

Qifan Yang, Dihong Huang, Yong Chen, and Ningyi Dai, *Senior Member, IEEE*

***Abstract*—Fine tuning the parameters is crucial for achieving high-performance power electronics converters. Traditionally, iterative testing using professional simulation tools has been a common approach. However, running the simulation model is time consuming, and online parameter optimization generates parameters specific to each operating condition. In this article, we propose a novel approach that combines artificial intelligence (AI)-aided parameter tuning with simulation using a data-driven empowered surrogate model. The surrogate model is trained using a dataset derived from 3000 simulation tests, enabling rapid parameter tuning with feedback on system performance within a time frame of less than 0.1 ms, even on devices with restricted computational capabilities. Moreover, comprehensive parameter optimization for multiscenarios can be achieved using the surrogate model. A case study focusing on the parameter tuning of the soft-open-point is provided, including a comparison with AI-aided autonomous online parameter tuning methods. The results demonstrate the effectiveness and efficiency of the proposed approach.**

***Index Terms*—Control parameter tuning, simulation, soft open point (SOP), surrogate model.**

I. Introduction

FOR power electronic converters, fine-tuned and well-designed control parameters are crucial to achieve satisfying performance. However, due to the nonlinear nature and high-order system dynamics of power electronic devices, it is challenging to systematically optimize control parameters and find optimal solutions. Conventional control parameter analysis involves transfer function design and linearization-based phase margin assessment and the optimization process relies on iterative manual simulations [1]. The main drawback of manual parameter tuning (MPT) is that relying on the established approximate model can lead to unpredictable errors, and variations in human expertise can greatly impact its efficiency. Therefore, exploring new parameter tuning methods that involve less human intervention and rely more on intelligent approaches may present a potential solution.

In recent years, artificial intelligence (AI) has been widely applied in the field of power electronics for design, control, and other aspects [2]. This includes the utilization of machine learning and meta-heuristic optimization methods [3]. Machine learning models, credited for their inherent strength of pattern recognition and nonlinear fitting, have been extensively utilized in the design of power electronics serving as surrogate models to improve the precision of theoretical modeling. A neural network (NN)-based optimal framework was proposed for the aim of designing the circuit parameters of a buck converter [4]. Zhang et al. [5] proposed an NN to map the control parameters to the system's pole. This work indicates that NN has the capability to map the nonlinear function in the power electronics area.

Meanwhile, metaheuristic methods, such as genetic algorithm (GA) and particle swarm optimization (PSO), utilizing general-purpose and high-level heuristics to iteratively explore and discover near-optimal solutions, have demonstrated superior performance in optimizing control parameters with less human expertise [6]. For instance, Naidu et al. [7] utilized a PSO algorithm to optimize the parameters of a proportional integral (PI) controller. A gray wolf optimizer was proposed in [8] to optimize a fractional-order PI controller for power factor correction. A hybrid wolf optimization algorithm was proposed to automatically adjust the controller's parameters of sliding mode direct torque control (SMDTC) for surface-mounted permanent magnet synchronous motors (SPMSMs) in [9]. The GA was proposed in [10] to optimize the sliding mode control.

The online NN training-based method, utilizing reinforcement learning, was proposed to design and optimize the PID controller [11], [12]. However, this kind of tuning method requires extensive online operation either on power electronic simulations or physical entities, taking relatively long convergence times to find the near-optimal solution and specific to single scenario. In order to achieve the optimal result in the static operation point, the simulations are usually running in the

Manuscript received 31 March 2024; revised 27 April 2024; accepted 30 April 2024. Date of publication 3 May 2024; date of current version 4 September 2024. This work was supported by the China Southern Power Grid Company, Ltd., under the project 030400KK52222021 (GDKJXM20222203). *(Corresponding author: Ningyi Dai.)*

Qifan Yang and Dihong Huang are with the State Key Laboratory of Internet of Things for Smart City and Department of Electrical and Computer Engineering, University of Macau, Macao 999078, China (e-mail: yc07464@um.edu.mo; yc37486@umac.mo).

Yong Chen is with the Guangdong Power Grid Corp, Zhuhai Power Supply Bureau, DC Power Distribution and Consumption Technology, Guangzhou 200235, China (e-mail: chenyong@gdzh.csg.cn).

Ningyi Dai is with the Zhuhai UM Science and Technology Research Institute and State Key Laboratory of Internet of Things for Smart City and Department of Electrical and Computer Engineering, University of Macau, Macao 999078, China (e-mail: nydai@um.edu.mo).

Color versions of one or more figures in this article are available at https://doi.org/10.1109/TPEL.2024.3396504.

Digital Object Identifier 10.1109/TPEL.2024.3396504

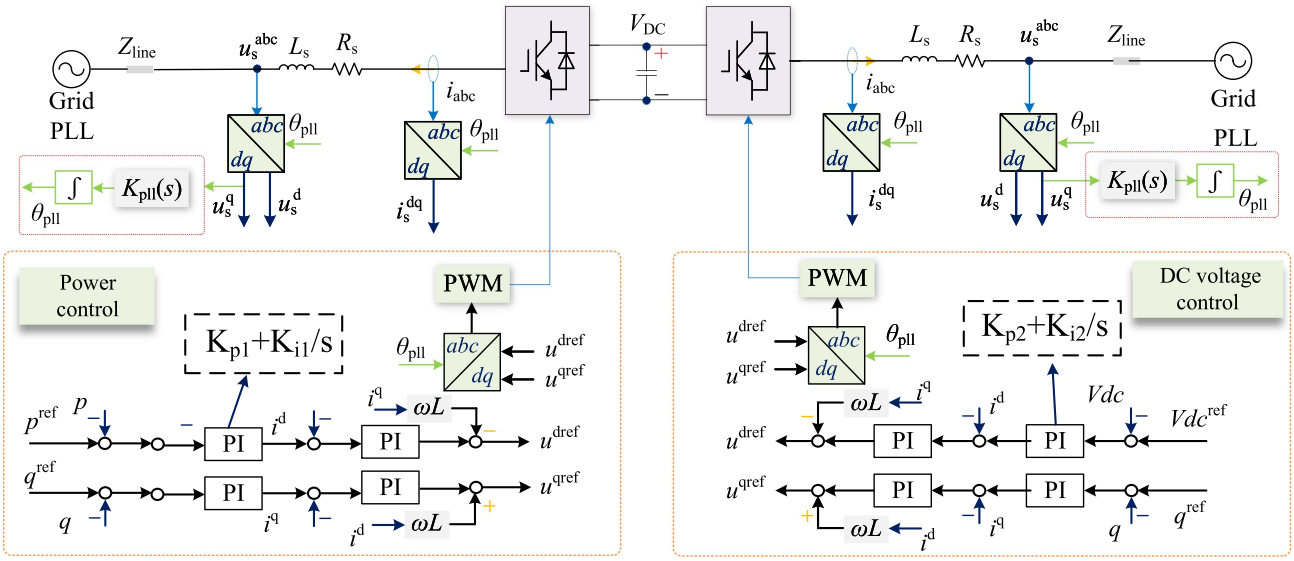

Fig. 1. Circuit and control system of SOP.

same scenario. However, when the static operating points of the system change, the obtained optimal parameters may no longer be applicable.

Considering the aforementioned limitations, the empowered and lightweight data-driven surrogate method is proposed to replace the simulation model. The core of this method lies in constructing a surrogate model based on historical data, where the input encompasses information on the static operating points as well as the decision variables that require optimization. After constructing the empowered and lightweight surrogate model, the optimization adopts an offline surrogate model parameter tuning (OSMPT) architecture, obtaining the optimization results through iterative execution of the surrogate model.

The soft-open-point (SOP), depicted in the Fig. 1, with the structure of two voltage source converters (VSCs), separately control the dc-link voltage and active power. The SOP has a back-to-back structure and is commonly utilized for achieving optimal power flow in medium-voltage distribution networks and microgrid systems, enabling the control of active power flow from one node to another [13]. The stability of the dc-side voltage of the SOP is a crucial factor during system operation [14], and its influence varies across different operating points [15]. Usually, a system-level dispatching algorithm generates the active power reference values for SOP from a few minutes to an hour [16]. Due to the characteristic of the SOP frequently changing the reference value of active power throughout the day [17], we adopted the SOP as the case study. The main contributions of this article are organized as follows.

1) An empowered and lightweight surrogate model-based comprehensive parameter optimization architecture is proposed to optimize the performance of SOP.
2) The proposed method employs a trained surrogate model to substitute real-time simulation in each iteration of parameter optimization. This approach significantly enhances the efficiency of parameter tuning.
3) The surrogate model incorporates the operation point feature and facilitates control parameter optimization for multiple scenarios, allowing for the consideration of the overall performance across all scenarios rather than just a single scenario.
4) The proposed architecture is compared with traditional online parameter tuning (OPT) architecture, demonstrating its superior advantage especially in multiscenario optimization.

To verify the precision of the proposed method, hardware-in-the-loop (HIL) experimental results are provided. HIL, which offers accuracy that bridges the gap between simulation and actual hardware, has been widely applied in the field of power electronics in recent years [18].

The rest of this article is organized as follows. The detailed introduction of the OPT and OSMP architecture is illustrated in the Section II. In Section III, the simulation results are provided. Experimental results is shown in Section IV. Finally, Section V concludes this article.

II. Architecture

In this section, we provide a detailed comparison of the differences between the two methods. The optimization task can be described as follows:

$$\begin{aligned} \min \quad & \sum_{i=1}^{n} t_{pi}(X) \text{ ms} \\ \text{s.t.} \quad & dV_i(X) < 0.05 \text{ pu} \\ & dP_i(X) < 10\ \% \end{aligned} \tag{1}$$

where i denotes the scenario number, for instance, every step change at different operating points can be seen as a scenario. t_{pi} is the peak time, and dP_i is the overshoot, of the active power of the power controlled VSC during a step change in its reference active power. dV_i is the max dc voltage deviation while the step change takes place during the scenario i. $X = [k_{p1}, k_{i1}, k_{p2}, k_{i2}]$, is the d-axis outer loop's PI parameters, highlighted in Fig. 1 . The task is to minimize the peak time and to

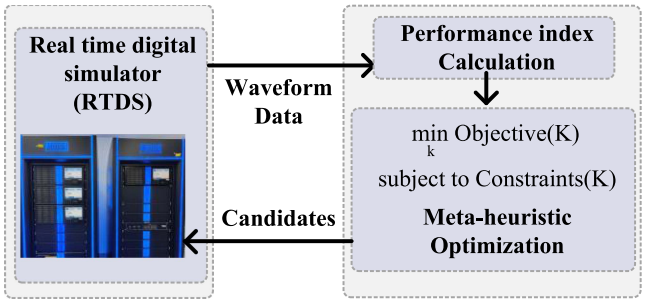

Fig. 2. Detailed process of OPT.

Algorithm 1: Genetic Algorithm for OPT and OSMPT.

Initialize population of $k_{p1}, k_{p2}, k_{i1}, k_{i2}$
Evaluate the fitness of each candidate by calculating t_{pi} and checking constraints dP_i and dV_i (For the OPT, by running the simulator. For OSMPT, calculating the neural networks' output.)
while termination condition not met **do**
  Select parents from the population based on fitness
  Perform crossover on parents to create offspring
  Apply mutation to offspring to vary $k_{p1}, k_{p2}, k_{i1}, k_{i2}$
  Evaluate the fitness of the new offspring by calculating t_p
  Check constraints dP_i and dV_i for each offspring
  Select individuals for the next generation
end while
return The best solution found for $k_{p1}, k_{p2}, k_{i1}, k_{i2}$

guarantee the overshoot and voltage fluctuation in an acceptable range. To control variables consistently, the GA is adopted as the optimizer with the same decision variables domain for its proven effectiveness compared with simulated annealing and ant colony optimization in handling nonconvex optimization problems with large search spaces and nonlinear constraints [10]. The optimization result analysis is conducted for both single-scenario and multiscenario settings. The implementation process of the GA on OPT and OSMPT is detailed in Algorithm 1.

A. OPT Architecture

The detailed process of the OPT is illustrated in Fig. 2 . This method establishes a loop connection between the simulator and the optimizer. In each iteration epoch, the optimizer generates candidate parameters and sends them to the real-time digital simulator (RTDS). The RTDS receives the parameters and updates the control model in simulation. The waveform data of the SOP is then sent back, and the performance indices are calculated. Subsequently, the optimizer generates a new group of candidates to be sent to the RTDS. This process runs iteratively until the OPT converges to the desired optimization task. It is important to note that during this process, the scenarios are typically fixed.

B. OSMPT Architecture

The detailed process of the OSMPT is depicted in Fig. 3. For the OSMPT architecture, the first step is to establish a surrogate model mapping decision variables to the objective function.

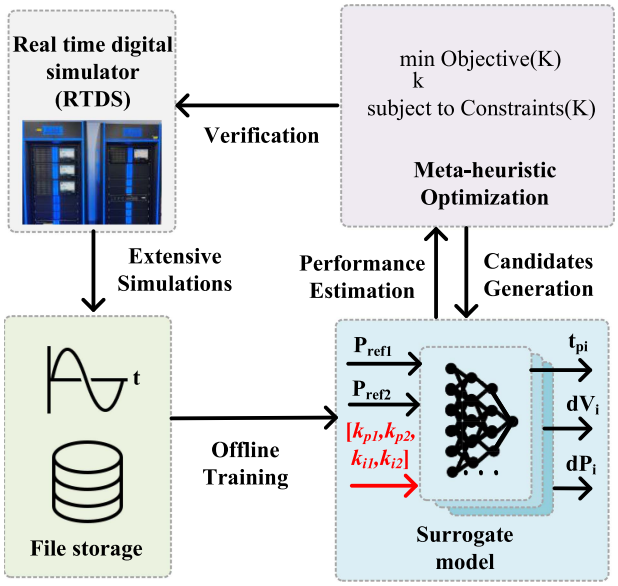

Fig. 3. Detailed process of OSMPT.

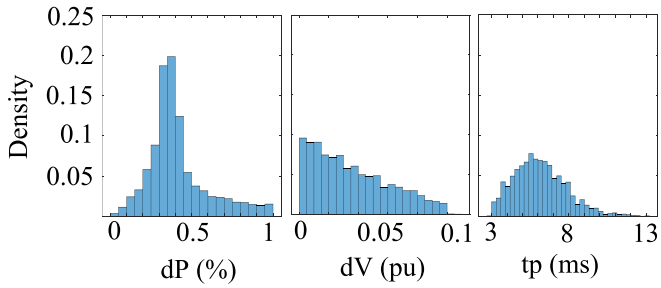

Fig. 4. Distribution of three performance index.

In this work, the training data for developing the surrogate model are obtained by collecting data from simulation models built in RTDS. The control parameters are generated randomly in a preset range. The preset range was determined by setting the lower boundary of control parameters to zero. The upper boundary is determined by considering both the stability margin and the typical range. k_{p1} and k_{p2} are from 0 to 3, k_{i1} is from 0 to 1, and k_{i2} is from 0 to 5. In this article, Pref1 means the initial active power reference value, while Pref2 is the active power reference after the step change. During the step change, the active power reference was changed from Pref1 to Pref2. The operating points are also generated randomly in a preset range from -3 to 3 MW. This range effectively narrows down the peak time to approximately 10 ms. Each time, one group of P_{ref1}, P_{ref2}, k_{p1}, k_{p2}, k_{i1}, and k_{i2} is generated and used in the simulation. Peak time, percentage overshoot, and max dc voltage deviation during this step-change of active power for a VSC are measured and recorded. Then, one group of training data is generated. RTDS/RSCAD allows users to write a script file to make it simulate all the cases automatically. The simulation software runs iteratively until the required number of cases is tested. The data are stored automatically in an Excel file. In this article, the dataset includes 3000 groups for training. The distribution of the three performance indices is depicted in Fig. 4. The x-axis

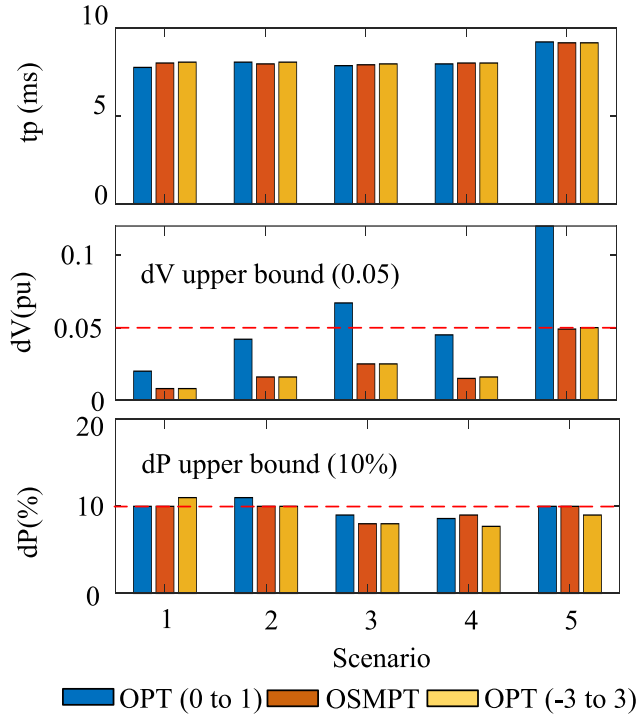

Fig. 5. Optimal results of OPT and OSMPT in multiple scenarios.

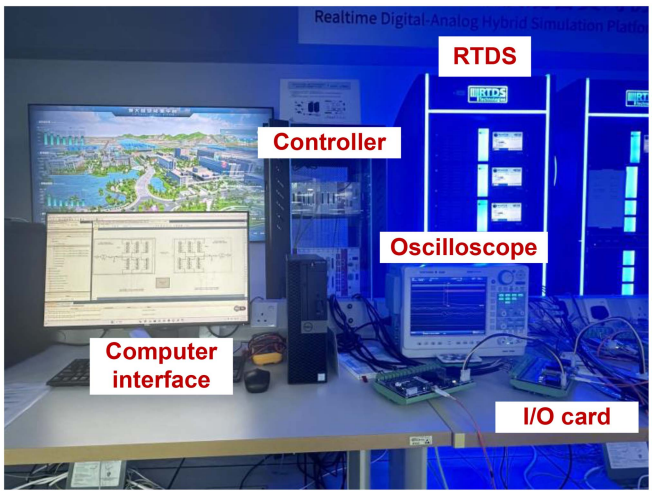

Fig. 6. Real-time hardware-in-loop platform.

represents specific numerical values. The y-axis represents the proportion of samples in a given numerical range relative to the total number of samples.

The feed-forward neural network is chosen as the surrogate model to map the P_{ref1}, P_{ref2}, k_{p1}, k_{p2}, k_{i1}, and k_{i2} to the peak time, overshoot, and max dc voltage deviation. Three NNs with a six-input-one-output structure are established, allowing flexible training and focused optimization for each performance index and mitigating the risk of mutual interference or conflicting objectives during the learning process [19]. Each NN is composed of two hidden layers, with each hidden layer containing 32 neurons, and the rectified linear unit (ReLU) function is utilized as the activation layer. The training process is implemented

TABLE I
PERFORMANCE COMPARISON OF THE THREE TRAINED NNS

Performance	tp	dV	dP
RMSE Value	0.2897	0.0042	0.0458
MAE Value	0.2019	0.0017	0.0242
R Square Value	0.971	0.972	0.938
Training Time	12.50s	11.13s	11.54s

TABLE II
SYSTEM CONFIGURATION OF SOP

System elements	Parameters	Value
VSC 1,2	Rated Power	10 MVA
	PCC nominal voltage	11kV
	Grid nominal frequency	50 HZ
	Number of SMs per arm	20
	SM Capacitance	100 mF
	Arm Inductance	0.006 H
DC bus	DC bus norminal voltage	$\pm$ 10 kV

with the Pytorch framework, and the Adam optimizer and mean squared error loss function are selected for training the NN. The learning rate is set to 0.01, and the maximum training epoch is set to 100. The training and validation sets were subjected to fivefold cross validation. The performance on the validation set and training time are listed in Table I, containing the root mean square error (RMSE), mean absolute error (MAE), and R square value. The NN is composed of adders and multipliers, which can be seen as a surrogate model of the simulation.

Based on the trained surrogate model, metaheuristic optimization is used to find the optimized parameters. Unlike the OPT architecture, the iteration process is conducted by the surrogate model. The NN consists of addition and multiplication operations, hence the computational burden of a single operation to get the performance is significantly lower than that of running one simulation. Compared to the time required for running a simulation (10 s is allotted to ensure that the system reaches an initial stable state), it is evident that the time needed for calculating the output of an NN (approximately 0.0001 s) is much smaller.

III. SIMULATION RESULTS

In this section, we adopt both OPT and OSMPT architecture in the single scenario and multiple scenarios. The first case applies a single scenario where the active power reference value increases from 0 to 1 MW. The number of simulation iterations are fixed, and the convergence results are observed over the same duration. The second case applies multiple scenarios and keeps the number of simulation runs constant for comparing the two methods. The system configuration of the studied system is listed in Table II, where the inner current loop control parameter is fixed. While SOP is assumed to be connected to strong grids on both sides, it is important to note that grid strength can vary within a certain range. A comprehensive study on the parameter optimization for weak grid scenarios will be conducted in future work.

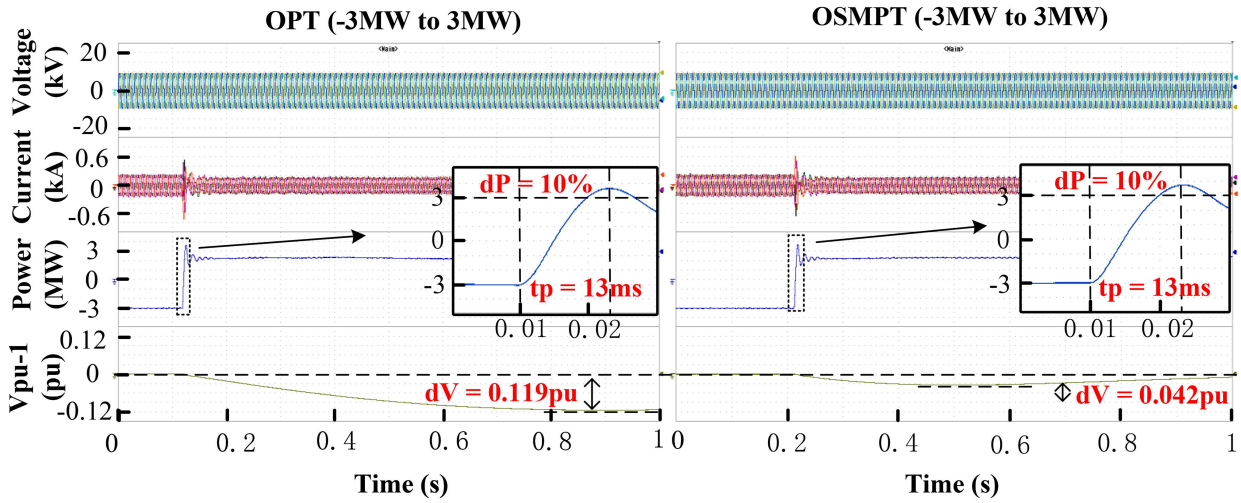

Fig. 7. HIL experimental results.

TABLE III
OPTIMAL RESULT IN SINGLE SCENARIO

Method	k_{p1}/k_{p2}	k_{i1}/k_{i2}	tp(ms)	dV(pu)	dp	Time
OPT	0.48 0.825	0.416 0.85	7.75	0.02	10%	8h
OSMPT	0.49 0.0589	0.589 0.839	7.8	0.035	9.8%	2.49s

TABLE IV
SCENARIOS OF THE ACTIVE POWER STEP CHANGE

Scenario	**1**	**2**	**3**	**4**	**5**
Pref1	0MW	1MW	2MW	-1MW	-3MW
Pref2	1MW	3MW	-1MW	-3MW	3MW

TABLE V
OPTIMAL RESULT OF OPT AND OSMPT

Method	**kp1**	**kp2**	**ki1**	**ki2**	**Time**	$\sum_{i=1}^{n} t_{pi}$
OPT(0 to 1)	0.480	0.825	0.416	0.850	8h	40.8
OSMPT	0.473	2.633	0.862	4.096	8.13s	41
OPT(-3 to 3)	0.684	2.888	0.165	3.896	8h	41.2

A. Comparison of Performance Metrics for the Two Methods Under Single Scenario

The comparison of two methods in the single scenario is listed in Table III. From the aforementioned table, it can be observed given the direct connection between the OPT architecture and the simulation, the results essentially meet the constraints' limitations, achieving an optimized outcome. The OSMPT architecture, due to precision loss in the data-driven modeling process, poses a certain risk of exceeding boundaries for voltage and active power. However, it is also observed that using the OSMPT method significantly reduces the time required for optimization, thereby substantially increasing the efficiency of the optimization process. The GA is implemented on a computer with Intel(R) Xeon(R) Gold 6140 2.30-GHz CPU with 64-GB memory. We utilized the RTDS Novacor2 for real-time digital simulations. The processor is based on the IBM POWER9 processor.

B. Comparison of Performance Metrics for the Two Methods Under Multiple Scenarios

In this section, we generated five scenarios to validate the effectiveness of the two architectures considering the typical operation range of the SOP [16]. Five different variations of active power step changes, ranging from 10% to 60% of SOP's rating, are tested. These settings are listed in Table IV. To ensure the consistency of variables, we employed a limit of 3000 times simulations. For OPT, this serves as a constraint to find the optimum value in a single scenario, while for OSMPT, 3000 datasets enable the construction of a model with higher accuracy.

Due to the characteristic of OPT's architecture, which can only operate at fixed working points, we executed the OPT optimization process separately under Scenarios 1 and 5. These two scenarios have a minimal step change from 0 to 1 MW and a maximal step change from -3 to 3 MW. Consequently, two groups of different control parameters are generated under each scenario, as listed in Table V. Each group of parameters was then applied to the other four scenarios in Table IV, and corresponding performance indices are shown in Fig. 5.

The OSMPT architecture is superior in its flexibility to modify the objective function and adapt to different scenarios. In this task, we refer back to (1), where we can set $n = 5$, such an operation does not contribute to the overall time consumption of the optimization process. The optimal result are also depicted in Fig. 5.

From Fig. 5, we can observe that the OPT architecture, optimized based on a single scenario, experiences dc voltage deviation and power overshoot exceeding their limits under multiple scenarios testing. For instance, in Scenarios 3 and 5, the dV of OPT (0 to 1) significantly exceeds the specified upper bound. In scenario 1, the percentage overshoot dP of OPT (-3 to 3) is out of constraint. It is important to note that, since parameter tuning was conducted under one specific

scenario, it is reasonable for some performance index to exceed the boundaries. This limitation is inherent to the OPT method. In contrast, the OSMPT architecture, which considers comprehensive optimization across multiple scenarios, performs more consistently at different step response sizes.

To enable the OPT method to achieve comprehensive optimization performance across different scenarios, another approach is to increase the number of simulation times. However, as the number of scenarios increases, the required number of simulation runs also increases linearly. On the contrary, for the OSMPT architecture, an increase in scenarios does not necessitate additional simulation resources.

Therefore, when operating under an identical number of simulations, the OSMPT architecture demonstrates enhanced efficiency considering multiple scenarios.

IV. Experimental Results

To validate the accuracy of the proposed optimization architecture on physical systems, we employed a HIL testing approach. The platform is shown in Fig. 6. The system is conducted using the RTDS, whereas the control system is in the RTU-BOX 204, which is equipped with DSP TMS320C28346.

We conducted validations using two sets of control parameters. Specifically, we tested the parameters optimized for the reference active power from -3 to 3 MW. For OPT $k_{p1} = 0.48$, $k_{p2} = 0.825$, $k_{i1} = 0.416$, and $k_{i2} = 0.85$, and for OSMPT, $k_{p1} = 0.473$, $k_{p2} = 2.633$, $k_{i1} = 0.862$, and $k_{i2} = 4.096$. The experimental result is depicted in Fig. 7. The obtained results align closely with the simulation depicted in Fig. 5.

V. Conclusion

This article proposed a data-driven-based comprehensive parameter optimization method for power electronics converters. Parameter optimization of the SOP is studied, focusing on achieving faster response times while ensuring dc voltage deviation and active power overshoot are within specific ranges. The traditional OPT architecture and the proposed OSMPT architecture were compared under single and multiple scenarios. Simulation and experimental results indicate that the proposed OSMPT architecture has a greater advantage in multiscenario optimization.

In this article, we assume that the RTDS simulations and offline training need to be conducted again when there are changes in the circuit structure and parameters. One issue we would like to highlight is that the trained data-driven model has acquired a substantial amount of information from the data. In cases where only minor changes are made, it may not be necessary to collect a large amount of training data again. Instead, techniques such as transfer learning and incremental learning can be employed to significantly enhance the efficiency of generating a new offline training model using limited amounts of new data. Furthermore, ensuring the stable operation of the grid and improving its performance under disturbances has become an increasingly important issue when designing control systems for converters. It is essential to thoroughly investigate the training of surrogate models and optimization tasks to handle more complex scenarios effectively. The aforementioned challenges will be studied in our future work to enhance the proposed method.

References

[1] A. G. Yepes, A. Vidal, J. Malvar, O. López, and J. Doval-Gandoy, "Tuning method aimed at optimized settling time and overshoot for synchronous proportional-integral current control in electric machines," *IEEE Trans. Power Electron.*, vol. 29, no. 6, pp. 3041–3054, Jun. 2014.

[2] S. Zhao, F. Blaabjerg, and H. Wang, "An overview of artificial intelligence applications for power electronics," *IEEE Trans. Power Electron.*, vol. 36, no. 4, pp. 4633–4658, Apr. 2021.

[3] S. E. De León-Aldaco, H. Calleja, and J. A. Alquicira, "Metaheuristic optimization methods applied to power converters: A review," *IEEE Trans. Power Electron.*, vol. 30, no. 12, pp. 6791–6803, Dec. 2015.

[4] X. Li, X. Zhang, F. Lin, and F. Blaabjerg, "Artificial-intelligence-based design for circuit parameters of power converters," *IEEE Trans. Ind. Electron.*, vol. 69, no. 11, pp. 11144–11155, Nov. 2022.

[5] C. Zhang, N. Mijatovic, X. Cai, and T. Dragičević, "Artificial neural network-based pole-tracking method for online stabilization control of grid-tied VSC," *IEEE Trans. Ind. Electron.*, vol. 69, no. 12, pp. 13902–13909, Dec. 2022.

[6] S. B. Joseph, E. G. Dada, A. Abidemi, D. O. Oyewola, and B. M. Khammas, "Metaheuristic algorithms for PID controller parameters tuning: Review, approaches and open problems," *Heliyon*, vol. 8, no. 5, 2022, Art. no. e09399.

[7] T. A. Naidu, S. R. Arya, and R. Maurya, "Multiobjective dynamic voltage restorer with modified EPLL control and optimized PI-controller gains," *IEEE Trans. Power Electron.*, vol. 34, no. 3, pp. 2181–2192, Mar. 2019.

[8] K. C. and U. M. G., "Design of gray wolf optimizer algorithm-based fractional order PI controller for power factor correction in SMPS applications," *IEEE Trans. Power Electron.*, vol. 35, no. 2, pp. 2100–2118, Feb. 2020.

[9] Z. Jin, X. Sun, G. Lei, Y. Guo, and J. Zhu, "Sliding mode direct torque control of SPMSMs based on a hybrid wolf optimization algorithm," *IEEE Trans. Ind. Electron.*, vol. 69, no. 5, pp. 4534–4544, May 2022.

[10] A. Kessal and L. Rahmani, "Ga-optimized parameters of sliding-mode controller based on both output voltage and input current with an application in the PFC of AC/DC converters," *IEEE Trans. Power Electron.*, vol. 29, no. 6, pp. 3159–3165, Jun. 2014.

[11] M. Gheisarnejad and M. H. Khooban, "An intelligent non-integer PID controller-based deep reinforcement learning: Implementation and experimental results," *IEEE Trans. Ind. Electron.*, vol. 68, no. 4, pp. 3609–3618, Apr. 2021.

[12] Z. Guan and T. Yamamoto, "Design of a reinforcement learning PID controller," *IEEE Trans. Elect. Electron. Eng.*, vol. 16, no. 10, pp. 1354–1360, Oct. 2021.

[13] M. Naderi, Y. Khayat, Q. Shafiee, T. Dragicevic, H. Bevrani, and F. Blaabjerg, "Interconnected autonomous ac microgrids via back-to-back converters–Part I: Small-signal modeling," *IEEE Trans. Power Electron.*, vol. 35, no. 5, pp. 4728–4740, May 2020.

[14] S. Ouyang, J. Liu, Y. Yang, X. Chen, S. Song, and H. Wu, "DC voltage control strategy of three-terminal medium-voltage power electronic transformer-based soft normally open points," *IEEE Trans. Ind. Electron.*, vol. 67, no. 5, pp. 3684–3695, May 2020.

[15] M. Car, V. Lešić, and M. Vašak, "Cascaded control of back-to-back converter dc link voltage robust to grid parameters variation," *IEEE Trans. Ind. Electron.*, vol. 68, no. 3, pp. 1994–2004, Mar. 2021.

[16] P. Li et al., "Coordinated control method of voltage and reactive power for active distribution networks based on soft open point," *IEEE Trans. Sustain. Energy*, vol. 8, no. 4, pp. 1430–1442, Oct. 2017.

[17] Q. Hou, G. Chen, N. Dai, and H. Zhang, "Distributionally robust chance-constrained optimization for soft open points operation in active distribution networks," *CSEE J. Power Energy Syst.*, to be published, doi: 10.17775/CSEEJPES.2021.02110.

[18] J. Chen, Y. Zhao, M. Wang, K. Wang, Y. Huang, and Z. Xu, "Power sharing and storage-based regenerative braking energy utilization for sectioning post in electrified railways," *IEEE Trans. Transport. Electrific.*, to be published, doi: 0.1109/TTE.2023.3295089.

[19] X. Liu, Y. Wang, X. Liu, T. Zhao, and P. Wang, "More efficient energy management for hybrid ac/dc microgrids with hard constrained neural network-based conversion loss surrogate models," *IEEE Trans. Smart Grid*, vol. 15, no. 3, pp. 2534–2552, Mar. 2024.